Category: Biological Sciences, Medical Sciences

Tumour suppressor role of phospholipase C epsilon in Ras-triggered cancers

Marta Martins[1], Afshan McCarthy[2], Rhona Baxendale[2], Sabrina Guichard[2], Lorenza Magno[3], Nicoletta Kessaris[3], Mona El-Bahrawy[4], Philipp Yu[5] and Matilda Katan[1*]

[1]Institute of Structural and Molecular Biology, Division of Biosciences, University College London, Gower Street, London WC1E 6BT, UK

[2]Division of Cancer Biology, Chester Beatty Laboratories, The Institute of Cancer Research, Fulham Road, London SW3 6JB, UK

[3]Wolfson Institute for Biomedical Research and Department of Cell and Developmental Biology, University College London, Gower Street, London WC1E 6BT, UK

[4]Department of Histopathology, Imperial College London, Hammersmith Hospital, DuCane Road, London W12 0HS, UK

[5]Institut für Immunologie der Philipps-Universität Marburg, Biomedizinisches Forschungszentrum, Hans Meerwein Str. 2, 35032 Marburg, Germany

*Corresponding author

Matilda Katan, Institute of Structural and Molecular Biology, Division of Biosciences, University College London, Gower Street, London WC1E 6BT, UK

E-mail: m.katan@ucl.ac.uk

Telephone Number: +44 (0) 207 679 1556

Key words: Ras oncogene, Phospholipase C epsilon, cancer models

Short Title: Tumour suppression by PLCε

Abstract

Phospholipase C epsilon (PLCε) has been characterized as a direct effector of Ras *in vitro* and in cellular systems; however, the role of PLCε in tumorigenesis and its link to Ras in this context remain unclear. To assess the role of PLCε in Ras driven cancers, we generated two new mouse strains: one carrying a targeted deletion of *Plce* (*Plce*$^{-/-}$) and the other carrying mutant alleles of *Plce* unable to bind to Ras (*Plce*$^{RAm/RAm}$). The *Plce*$^{-/-}$ and, to a lesser degree, *Plce*$^{RAm/RAm}$ transgenic mice exhibited increased susceptibility to tumour formation in the two-stage skin carcinogenesis protocol revealing a tumour suppressor function for this PLC. This also suggests that in this context Ras binding in part regulates functions of PLCε. Although significant differences were not seen in the LSL-Kras^{G12D} non-small cell lung carcinoma model, downregulation of PLCε was found in animal tumours and in cellular systems following expression of the oncogenic Ras. An inhibitory impact of PLCε on cell growth requires intact lipase activity and is likely mediated by protein kinase C enzymes. Further cellular studies suggest involvement of histone deacetylase in the mechanism of PLCε downregulation. Taken together, our results show for the first time a tumour suppressor role for this PLC in animal models and together with observations of marked downregulation in colorectal, lung and skin tumours, suggest its use as a biological marker in cancer.

Statement

Ras oncogens have been implicated in high proportion of cancers. However, selective treatment for Ras oncogenes is not yet available and components that could mediate Ras functions are being extensively assessed as alternative targets. For some potential targets, such as phospholipase Cepsilon, it is not clear how they contribute to tumor development. Here we provide several lines of experimental evidence that support a tumour suppressor function of PLCepsilon, contrasting a positive role of several other well-defined effectors of Ras. Our results show a tumour suppressor role for this PLC in animal models and describe its impact on cell proliferation. Together with observations of marked downregulation in several types of tumours, this suggests its use as a biological marker in cancer.

\body **Introduction**

Activating mutations in the Ras subfamily of small GTPases contribute to the formation of a large proportion of human tumours (1). However, selective treatment for Ras oncogenes is not yet available in the clinic and components that could mediate generation and progression of tumours by Ras are being extensively assessed as alternative targets. These include direct signalling effectors (such as Raf-kinase, PI3-K and RalGDS) (2-4), recently identified Ras-binding protein (PDEδ) (5), as well as components less directly linked to Ras or necessary for Ras oncogene-dependent cancer cell survival (for example, Ral, Cdk4, GATA, TBK1) (6-9). Approaches for evaluating their role *in vivo* are based on mouse models for Ras-triggered cancers. In addition to a two-stage chemical carcinogenesis model where a carcinogen (DMBA) generates activating mutations in Hras, other models, including lung and pancreatic cancer, have been developed based on inducible expression of Kras oncogene (10, 11). By applying these strategies and models to strains with ablated expression of a specific component or using specific inhibitors, it was possible to assess the requirement or contribution of each component in Ras triggered-malignancies. Some of the well-known direct effectors of Ras have been found necessary for tumour formation; in their absence tumour generation and progression is attenuated or absent. Examples include the requirement for c-Raf in Kras oncogene-driven non-small cell lung carcinoma (NSCLC) (4), PI3K p110α in NSCLC and in two-stage skin cancerogenesis (3) and Ral GDS in the same Hras oncogene-driven skin cancer model (2). In some instances, for example for PI3K, it was also possible to assess the requirement for a Ras-binding domain (RA) by generating alleles encoding p110α variants deficient in Ras-binding (3). However, not all proteins implicated in direct binding to Ras appear to have a positive role in Ras oncogene-driven tumours or tumours caused by other factors. For example, depletion of some members of the Ras Association Doman Family (rassf), such as Rassf1A, enhanced tumour formation in mice (12).

PLCε is a multifunctional signalling protein, incorporating both phospholipase C (PLC) and guanine nucleotide exchange factor (GEF) activities (13, 14). Importantly, and in common to several direct effectors of Ras, it has an RA domain that binds several Ras GTPases including oncogenic Kras and Hras (15). The main insights into *in vivo* functions of PLCε have been obtained using two different transgenic mouse strains, one with an in-frame deletion within the PLC catalytic domain ($Plce1^{\Delta X/\Delta X}$) and the other lacking PLCε expression

(*Plce1*$^{-/-}$) (16). While in both cases mice were viable, some notable differences in their phenotype, in particular related to heart morphology, have been observed. In assessing functions related to cancer, however, only *Plce1*$^{\Delta X/\Delta X}$ transgene-where the link between PLCε and a phenotype could be more difficult to interpret- has been used so far (16, 17). Some of these studies have suggested that the function of PLCε could be required for immune responses associated with the skin chemical cancerogenesis and colorectal models (18, 19). However, in the case of another skin cancer, caused by UVB light, that also triggers inflammation (20), such an overall positive role of PLCε was not seen. Furthermore, several studies based on analysis of human colorectal tumours (21-23) show markedly reduced levels of PLCε and indicate a cancer suppressing functions of PLCε rather than a positive role in generation and progression of tumours. Due to these apparent discrepancies, it is necessary to further scrutinize the role of PLCε in a more comprehensive study, including use of different *Plce1*transgenes.

We here describe generation of two new *Plce1* transgenic strains and their analysis in Ras-triggered cancers that, together with cellular studies and information for expression in human tumours, provide evidence for tumour suppressor role of PLCε.

Results

Generation and characterization of transgenic mice

To study the role of PLCε and its signalling links to Ras GTPases *in vivo*, we generated two new transgenic strains. *Plce* null mice (*Plce*$^{-/-}$) were generated by disruption of exon 2 of *Plce* and the introduction of a frameshift termination codon in exon 3, therefore preventing the expression of any functional domains of PLCε (Fig. 1A and B). The variant deficient in Ras-binding (*Plce*$^{RAm/RAm}$) was generated by introduction of three point mutations (R2130L, K2151E and Y2154L) into exon 29 and 30 of *Plce* allele (Fig. 1 B, right); these point mutations were previously shown to completely disrupt Ras binding to the RA2 domain of PLCε (15). *Plce*$^{-/-}$ and *Plce*$^{RAm/RAm}$ mice were bred to homozygosity exhibiting the expected Mendelian ratio (Fig. 1C). Homozygotes were fertile and showed normal life span and development.

Initial conformation for homologues recombination in ES cells was obtained by Southern blot analysis (Supplemental Fig. S1A). The excision of exon 2 in the *Plce*$^{-/-}$ mice

was confirmed by RT-PCR of various organs using primers for exon 2-3 (Fig. 1D, top). Point mutations generated in exon 29 and 30 of *Plce*$^{RAm/RAm}$ were verified in different organs based on the presence of specific restriction sites (Fig. 1D, bottom). In addition, the absence of PLCε expression was confirmed by Western blotting of protein extracts from selected organs and mouse embryonic fibroblasts (MEF) (Supplemental Fig. S1B and C). To access whether other PLCs would compensate for the absence of the *Plce* gene, protein extracts from *Plce*$^{+/+}$ and *Plce*$^{-/-}$ MEFs were used for Western blotting and showed no significant difference of expression of other PLCs (Supplemental Fig. S1C).

Two-stage chemical skin carcinogenesis

Before applying the two-stage chemical charcinogenesis protocol we analysed the skin from *Plce*$^{+/+}$, *Plce*$^{-/-}$ and *Plce*$^{RAm/RAm}$ mice and verified the absence of PLCε expression in the null mice and similar levels of expression in *Plce*$^{+/+}$and *Plce*$^{RAm/RAm}$ mice (Fig. 2A). We also confirmed PLCε expression in the epidermis and hair follicles of the dermis but not in the dermis itself (Supplemental Fig. S2A and S3B), as suggested previously (24).

For the two-stage chemical skin carcinogenesis model, driven through Hras signalling, *Plce*$^{+/+}$, *Plce*$^{-/-}$ and *Plce*$^{RAm/RAm}$ mice were backcrossed to FVB for 6 generations and cohorts of mice were treated with one single application of DMBA, to initiate oncogenic mutation on the *Hras* gene, and weekly applications of TPA, to promote clonal expansion of the initiated cells, for 18 weeks. Three tumours of each genotype were tested for the activating mutations at the 61st codon of *Hras* (25) and all tumours were found to carry the activating mutations, irrespective of the *Plce* genetic background (Supplemental Fig. S3A).

As shown in Fig. 2B, our results clearly show that the loss of PLCε leads to a significant increase in tumour burden compared to the wild type control mice. Similarly, *Plce*$^{RAm/RAm}$ mice also exhibited increase in tumour burden when compared to the wild type, suggesting that absence of signalling mediated by the RA2 domain of PLCε increases susceptibility to tumour development; however, mice with a total absence of PLCε exhibited an aggravated phenotype (Fig. 2B). We also excluded the possibility that the enhancement in tumour development was due to a reduction in apoptosis (Supplemental Fig. S3C).

When tumour volume was assessed at 13 weeks of treatment, *Plce*$^{-/-}$ mice had significantly bigger tumours than those seen in the wild type while no significant difference was seen between *Plce*$^{+/+}$ and *Plce*$^{RAm/RAm}$ (Fig. 2C). This suggests that RA2 domain could contribute to suppression of tumour formation without significantly affecting tumour growth.

In contrast, complete ablation of PLCε has an effect on both processes, affecting number and size of tumours.

Unexpectedly, the survival rate of the *Plce*$^{-/-}$ mice was drastically affected during the treatment (Fig. 2D). Our initial experiments performed on a different, C57Bl/6J-FVB (F1) mixed background (Supplemental Fig. S3 B and C), however, suggest that the FVB genetic background is affecting the survival of *Plce*$^{-/-}$ mice shown in Fig. 2D, rather than *Plce*$^{-/-}$ genotype *per se*. In C5Bl/6J-FVB background we have shown a similar increase in tumour burden in the *Plce*$^{-/-}$ mice (Supplemental Fig. S3B) but the survival of *Plce*$^{-/-}$ mice was not affected by the DMBA/TPA treatment (Supplemental Fig. S3C). It is, however, currently not possible to make clear inferences from these observations. C57BL/6 mice, which are relatively resistant to TPA skin tumor formation, have a number of not yet defined genetic loci which influence tumor susceptibility in the two-stage skin carcinogenesis model (26-28). Although to our knowledge, FVB vs C57BL/6 outcrossing to identify susceptibility genes has not been done, our data suggest that in the F1 (FVBxC57BL/6) generation a C57BL/6 derived "tumor survival" allele is present which could be associated with PLCε tumour suppressor or other roles relevant for tumour formation.

We also examined epidermal hyperplasia in TPA-treated skin in order to determine the potential effect of PLCε in the second proliferative step of the two chemical carcinogenesis protocol. Initial measurements of the skin thickness on day 2 showed that a single topical application of TPA at 10 μg induced thickening of the epidermis in all genotypes (from 19.3 ±1.8 μm to 39.3 ±3.5 μm in *Plce*$^{+/+}$, from 19.3 ±1.2 μm to 44.1 ±2.9 μm in *Plce*$^{RAm/RAm}$ and from 24.1 ±4.1 μm to 45.4 ±5.7 μm in *Plce*$^{-/-}$ mice). The measurements also suggested some thickening of the epidermis in *Plce*$^{-/-}$ mice compared to the wild-type under control conditions. This was further supported by data for the rate of cell proliferation in the vehicle or TPA treated skin using immunohistochemistry for Ki67 (Fig. 2E and Supplemental Fig. S4). TPA treatment of *Plce*$^{+/+}$ and *Plce*$^{RAm/RAm}$ induced an increase in the number of proliferative cells in the epidermis compared to the vehicle treated, control skin. TPA treatment also induced an increase in epidermal proliferation in the *Plce*$^{-/-}$ skin, however this increase was smaller than that seen in the *Plce*$^{+/+}$ and *Plce*$^{RAm/RAm}$ mice (Fig. 2E) and this appears to be due to the fact that there is a higher level of basal proliferation in the *Plce*$^{-/-}$ skin compared to the wild type skin (Fig. 2E, $P < 0.05$). These findings, revealing prolonged

higher basal proliferation rate of *Plce*$^{-/-}$ skin, are consistent with the results showing greater tumours in the *Plce*$^{-/-}$ mice compared to the other genotypes (Fig. 2C).

Analysis of skin tumours: PLCε downregulation

To investigate the level of expression of PLCε in the tumours, we analysed four tumours of four different mice of each genotype and compared these to untreated animals. The results showed a significant decrease in PLCε expression in the *Plce*$^{+/+}$ and *Plce*$^{RAm/RAm}$ tumour samples compared to normal skin, close to the level seen in the *Plce*$^{-/-}$ skin (Fig. 3A). This result seems to be in keeping with a putative tumour suppressor function of this PLC. To further investigate if Hras could directly down-regulate PLCε in tumours, primary MEFs from *Plce*$^{+/+}$ and *Plce*$^{RAm/RAm}$ embryos were first immortalized with retrovirus expressing a dominant negative form of the tumour suppressor protein p53 and subsequently transformed with the activated Hras mutant retrovirus (p53DD+HrasV12), or only transformed with HrasV12 retrovirus (HrasV12) (Fig. 3B). The data show that HrasV12 completely abrogates expression of the WT and RAm PLCε in cell culture. Furthermore, these data also suggest an epigenetic silencing of the *Plce* gene mediated by Hras that is independent of the Ras-binding domain. To examine the epigenetic regulation of this repression, the above immortalized and transformed MEFs were treated with the DNA methylation inhibitor 5-Aza-2'-Deoxycytidine (AZA) or with the histone deacetylase inhibitor Trichostatin A (TSA). Interestingly, TSA seems to increase or completely restore the expression of PLCε in HrasV12 and p53DD+HrasV12 transformed cells, respectively (Fig. 3C). Cellular differences between primary or immortalized cells may be the reason why MEFs expressing HrasV12 respond differently to TSA treatment in terms of PLCε expression. Unexpectedly, treatments with AZA seem to have a negative effect on PLCε expression despite restoring expression of Fas (Supplemental Fig. S5), one of the best characterized target of hypermethylation in Ras transformed cells (29). Thus, it appears that in MEFs histone deacetylases (HDAC) most likely mediate the down-regulation of PLCε. Similar results to those observed for *Plce*$^{+/+}$ MEFs (Figure 3C) were seen for the *Plce*$^{RAm/RAm}$ allele when using TSA and AZA (Supplemental Fig. S5A). Varying growth conditions and prolonged stimulations of MEFs did not affect expression levels of PLCε (Supplemental Fig. S5B and C).

To further analyse expression levels of PLCε during DMBA-TPA treatment we crossed our C57Bl/6J mice with a background known to be more resistant to the DMBA-TPA

treatment, the DBA mice, enabling us to slow down the tumourigenesis process and study treated skin that did not develop tumours. Wild type F1 mice (C57Bl/6J-DBA) were treated as previously and non-treated skin, treated skin and tumours were analysed at week 13 of the DMBA-TPA treatment. The three mice analysed showed an 80% downregulation of PLCε in treated skin (in the absence of lesions) compared to untreated (ventral) skin (Fig 3.D). This suggests that the down-regulation of PLCε also occur prior to tumour formation and is probably mediated by the TPA-promotion step. Overall, these results propose that activated mutations in the *Hras* gene can directly downregulate PLCε in cells, however, continuous skin treatment with TPA also down-regulates PLCε prior to tumour formation.

Our further experiments also suggested that exogenous expression of the wild-type PLCε in *Plce*$^{-/-}$ MEFs resulted in a reduction in cell proliferation; this effect seems to be dependent on intact lipase activity (Supplemental Fig. S6A). Consistent with this, re-expression of PLCε corresponded to an increase in PKC activity (as assessed by phosphorylation of PKC and its substrate MARCKS) (Supplemental Fig. S6B and C). As shown in Fig. S6D, we observed similar changes in pre-cancer skin from *Plce*$^{-/-}$ mice that is characterized by higher rate of proliferation (Fig. 2E). This suggests that the predominant mechanism that impacts on cell proliferation is mediated by PKC; isozymes previously linked to growth inhibition such as PKCδ or PKCη (30), are likely to be involved.

Kras driven lung tumour development

To further investigate the tumour suppressor function of PLCε, we used the conditional LSL-*Kras*^{G12D} NSCLC model. PLCε expression is highest in the lung (Fig. 4A) and *in situ* hybridization of the wild type lung shows ubiquitous expression of PLCε in this tissue (Supplemental, Fig. S2B). In this model, lung tumour initiation is synchronously induced by a single infection with an AdCre virus, which leads to the removal of the transcriptional stop element and activation of the oncogenic *Kras*^{G12D} allele. C57Bl/6J *Plce*$^{+/+}$, *Plce*$^{-/-}$ and *Plce*$^{RAm/RAm}$ mice were crossed with the *LSL-Kras*^{G12D} mouse and 6 week-old mice were infected with AdCre by intranasal instillation. Animals were sacrificed 23/24 weeks after AdCre infection and histological analysis of the lungs revealed similar tumour burden and tumour grade distribution among all genotypes (Fig. 4B-E). We quantified tumour burden by analysing the number of lesions per lung and measuring the tumour-to-lung area ratio (T/L) which revealed no significant difference between the genotypes (Fig. 4B and C).

Malignancy was assessed by counting the number of solid nodules and fraction of animals having solid tumours per genotype, which also did not show any significant difference between the genotypes (Fig. 4D and E).

PLCε expression (assessed by qPCR) was analysed in the whole, wild type untreated lungs and lungs from mice 26 weeks after AdCre infection showing 38% reduction (Fig. 4F). *In vitro* analysis of *LSL-Kras^{G12D}* MEFs showed a rapid down-regulation of PLCε after AdCre infection; 50% of PLCε reduction 6 days after AdCre infection (Fig. 4G). These results indicate that in the NSCLC model, where initiation of Kras^{G12D} expression is synchronised and a rapid down-regulation of PLCε is seen in Kras^{G12D} expressing MEFs, the *Plce$^{-/-}$* genotype does not have an effect on tumour burden in the lung. Effectively, Kras^{G12D} is likely to convert wild type cells into cells completely lacking PLCε as in *Plce$^{-/-}$* genotype.

PLCε downregulation in human lung tumours and cell lines

To investigate whether PLCε would also be down-regulated in human lung tumours, we have probed a commercial cancer-profiling array containing cDNA from 21 pairs of normal/tumour patient samples. Quantitative analysis revealed that in about 73 % of tumours there was a decrease in PLCε mRNA compared to the normal tissues (Fig. 4H). The reduction of expression was within a range of 2 to 9.3 fold. Human epithelial carcinoma cell lines were also analysed for expression of PLCε. Among several non-small lung cancer cell lines, H358 and H460 cells showed comparatively low or no PLCε expression as assessed by Western blotting or RT-PCR (Fig. 4J). Notably, TSA treatment of these cell lines resulted in an increase in the level of PLCε (Fig. 4J, left panels).

Discussion

Here we provide several lines of experimental evidence that support a tumour suppressor function of PLCε, contrasting a positive role of several other well-defined effectors of Ras in Ras-triggered generation and progression of tumours. We have found an increase in susceptibility to skin tumour formation in *Plce$^{-/-}$* mice in response to DMBA/TPA (Fig. 2) and down-regulation of PLCε in skin and lung tumours as well as in cellular models following expression of oncogenic Ras (Fig. 3 and 4). In addition to Ras-driven animal tumours, the reduction in PLCε expression levels was also observed in human lung adenocarcinomas (Fig. 4). The down regulation of PLCε is likely to account for apparent

inconsistencies between the skin (increase in tumours) and lung model (no change in tumour burden) (Fig. 2 and 4) that can be due to an extensive, synchronized and more rapid down-regulation in the latter.

While the effect of PLCε-deficiency on tumour formation in mice differs from ablation of several other Ras effectors (Raf, PI3K or RalGDS; (2-4)), it shows similarities with protein kinase Cη (PKCη) knock out strain when analysed by two-stage chemical carcinogesis (30). This novel PKC isoform, regulated by PLC-generated diacylglycerol, is highly expressed in the skin. As in the case of PLCε-deficiency (Fig. 2), the lack of this enzyme in *Prkch*$^{-/-}$ mice resulted in an increased susceptibility to skin tumor formation compared to the wild-type. Interestingly, in both cases a suppressive effect on TPA induced epidermal hyperplasia could be one of the factors involved in the control of tumour formation; PKCη-deficient mice have prolonged epidermal hyperplasia (30) and our data suggest that the high proliferative rate of basal cells in the epidermis of the *Plce*$^{-/-}$ mice may be closely associated with increased tumour growth (Fig. 2). We also note that our data from the application of the two-stage chemical carcinogenesis model differ from previous observations obtained using another, *Plce1*$^{\Delta X/\Delta X}$ transgene (24); this difference is likely caused by different approaches in interfering with functions of this complex protein.

Analysis of *Plce*$^{RAm/RAm}$ mice, the strain where binding of a subset of Ras family GTPases to the PLCε RA2 domain is abolished, demonstrated that regulatory interactions mediated by the RA2 domain contribute to tumour suppressive roles of PLCε. An increase in number of skin tumours was observed in *Plce*$^{-/-}$ and *Plce*$^{RAm/RAm}$ mice; an increase in tumour volume and epidermal proliferative rate, however, was only seen in *Plce*$^{-/-}$ mice (Fig. 2). Notably, down-regulation of PLCε was independent of functional RA2 domain and both the wild type PLCε and PLCε with RAm mutations were similarly down-regulated (Fig. 3). This supports the possibility that tumour suppressive functions of PLCε involve RA2-mediated regulatory interactions-notably with the oncogenic Ras- at least at early stages (that influence tumour generation). However, at later stages in tumorigenesis down-regulation of PLCε becomes prominent.

It has been well established that Ras driven cancers exhibit a complex picture of up-regulated and down-regulated gene expression compared to normal cells. The best-characterized mechanisms for downregulation involve epigenetic silencing by promoter hypermethylation (29). Interestingly, this may not be the prevalent mechanism for

downregulation of PLCε as we show that PLCε re-expression in our cellular systems can be achieved by the histone deacetylase inhibitor (TSA) rather than the DNA methylation inhibitor (AZA) (Fig. 3 and 4).

To our knowledge, the expression levels of PLCε have not been previously analysed in skin or lung human tumours and we provide the first evidence for down-regulation of PLCε in these tumour types. Nevertheless, data from several previous reports demonstrate a great reduction of PLCε expression in another type of human tumour, colorectal cancer (CRC), and suggest some further similarities with observations presented here. Results from Sorli et al. demonstrated significantly reduced mRNA expression levels in colon and rectum cancer samples and several colon cancer cell lines expressing Ras oncogene (21). Wang and colleagues reported a frequency of 36% loss of heterozygosity of 10q23 (where *PLCE1* is located) and down-regulation of PLCε in 21/50 colorectal cancer samples compared with matched normal tissue (22, 31). Recently, Danielsen et al. performed a comprehensive statistical analysis of data for CRC and normal mucosa (from different microarray platforms) and subsequent validation of the main findings (23). They have demonstrated that PLCε is one of the most significantly down-regulated components, with the expression levels decreasing with more advanced stages, indicating that the repression of *PLCE1* gene facilitates cancer progression. Notably, this study also reported strong association between low expression of PLCε and *KRAS* mutations (P=0.006) but not with mutations in *BRAF*, *PIK3CA* or *PTEN*. Furthermore, previous studies of colorectal cell lines and ectopic overexpression of PLCε (in cells with low endogenous levels of this PLC) have reported inhibition of tumour cell proliferation, increased apoptosis, reduced number of colonies formed in cell culture and reduced tumour formation in a xenograft model *in vivo* (21, 22), all consistent with a tumor suppressive role for *PLCE1* gene.

Taken together with previously published observations, our comprehensive study, including animal models, suggests that PLCε has tumour suppressive functions in the formation of several cancer types (including CRC, lung and skin), and that its marked down-regulation could be a useful biological marker in their assessment and treatment.

Materials and Methods

Generation of Plce$^{-/-}$ and Plce$^{RAm/RAm}$Mice. Generation of PLCε transgenic mice was based on a standard homologous recombination strategy using stem cell manipulation. For details, see SI Material and Methods.

Cancer Models and Analysis of Tumours. Skin tumour formation was based on DMBA/TPA two-stage carcinogenesis protocol and lung tumours were generated by lung infection with adenovirus (Ad-Cre) on *LSL-Kras^{G12D}*background. Tumours were analysed by qRT-PCR, histopathology and immunohistochemistry, in situ hybridization and cancer profiling array. See SI Material and Methods for details.

Cell culture. Generation and culture of MEFs and other cell lines and their further analysis was carried out as described in SI Material and Methods.

Acknowledgments

We are grateful to Georgia Zoumpoulidou and Sibylle Mittnacht for regents and Bradley Spencer-Dene for help with *in situ* hybridization. We thank Chris Marshall for helpful discussions. Work in MK's laboratory has been funded by Cancer Research UK and Wellcome Trust.

REFERENCES

1. Pylayeva-Gupta Y, Grabocka E, & Bar-Sagi D (2011) RAS oncogenes: weaving a tumorigenic web. *Nat Rev Cancer* 11(11):761-774.

2. Gonzalez-Garcia A, *et al*. (2005) RalGDS is required for tumor formation in a model of skin carcinogenesis. *Cancer Cell* 7(3):219-226.

3. Gupta S, *et al*. (2007) Binding of ras to phosphoinositide 3-kinase p110alpha is required for ras-driven tumorigenesis in mice. *Cell* 129(5):957-968.

4. Blasco RB, *et al*. (2011) c-Raf, but not B-Raf, is essential for development of K-Ras oncogene-driven non-small cell lung carcinoma. *Cancer Cell* 19(5):652-663.

5. Zimmermann G, *et al*. (2013) Small molecule inhibition of the KRAS-PDEdelta interaction impairs oncogenic KRAS signalling. *Nature* 497(7451):638-642.

6. Kumar MS, *et al*. (2012) The GATA2 transcriptional network is requisite for RAS oncogene-driven non-small cell lung cancer. *Cell* 149(3):642-655.

7. Peschard P, *et al*. (2012) Genetic deletion of RALA and RALB small GTPases reveals redundant functions in development and tumorigenesis. *Curr Biol* 22(21):2063-2068.

8. Puyol M, *et al*. (2010) A synthetic lethal interaction between K-Ras oncogenes and Cdk4 unveils a therapeutic strategy for non-small cell lung carcinoma. *Cancer Cell* 18(1):63-73.

9. Barbie DA, *et al*. (2009) Systematic RNA interference reveals that oncogenic KRAS-driven cancers require TBK1. *Nature* 462(7269):108-112.

10. O'Hagan RC & Heyer J (2011) KRAS Mouse Models: Modeling Cancer Harboring KRAS Mutations. *Genes Cancer* 2(3):335-343.

11. Perez-Mancera PA, Guerra C, Barbacid M, & Tuveson DA (2012) What we have learned about pancreatic cancer from mouse models. *Gastroenterology* 142(5):1079-1092.

12. Tommasi S, *et al*. (2005) Tumor susceptibility of Rassf1a knockout mice. *Cancer Res* 65(1):92-98.

13. Bunney TD & Katan M (2006) Phospholipase C epsilon: linking second messengers and small GTPases. *Trends Cell Biol* 16(12):640-648.

14. Bunney TD & Katan M (2011) PLC regulation: emerging pictures for molecular mechanisms. *Trends Biochem Sci* 36(2):88-96.

15. Bunney TD, *et al*. (2006) Structural and mechanistic insights into ras association domains of phospholipase C epsilon. *Mol Cell* 21(4):495-507.

16. Smrcka AV, Brown JH, & Holz GG (2012) Role of phospholipase Cepsilon in physiological phosphoinositide signaling networks. *Cell Signal*.

17. Bunney TD & Katan M (2010) Phosphoinositide signalling in cancer: beyond PI3K and PTEN. *Nat Rev Cancer* 10(5):342-352.

18. Ikuta S, Edamatsu H, Li M, Hu L, & Kataoka T (2008) Crucial role of phospholipase C epsilon in skin inflammation induced by tumor-promoting phorbol ester. *Cancer Res* 68(1):64-72.

19. Li M, Edamatsu H, Kitazawa R, Kitazawa S, & Kataoka T (2009) Phospholipase Cepsilon promotes intestinal tumorigenesis of Apc(Min/+) mice through augmentation of inflammation and angiogenesis. *Carcinogenesis* 30(8):1424-1432.

20. Oka M, *et al*. (2010) Enhancement of ultraviolet B-induced skin tumor development in phospholipase Cepsilon-knockout mice is associated with decreased cell death. *Carcinogenesis* 31(10):1897-1902.

21. Sorli SC, Bunney TD, Sugden PH, Paterson HF, & Katan M (2005) Signaling properties and expression in normal and tumor tissues of two phospholipase C epsilon splice variants. *Oncogene* 24(1):90-100.

22. Wang X, *et al*. (2012) Phospholipase C epsilon plays a suppressive role in incidence of colorectal cancer. *Med Oncol* 29(2):1051-1058.

23. Danielsen SA, *et al*. (2011) Phospholipase C isozymes are deregulated in colorectal cancer--insights gained from gene set enrichment analysis of the transcriptome. *PLoS One* 6(9):e24419.

24. Bai Y, *et al*. (2004) Crucial role of phospholipase Cepsilon in chemical carcinogen-induced skin tumor development. *Cancer Res* 64(24):8808-8810.

25. Finch JS, Albino HE, & Bowden GT (1996) Quantitation of early clonal expansion of two mutant 61st codon c-Ha-ras alleles in DMBA/TPA treated mouse skin by nested PCR/RFLP. *Carcinogenesis* 17(12):2551-2557.

26. Hennings H, *et al*. (1993) FVB/N mice: an inbred strain sensitive to the chemical induction of squamous cell carcinomas in the skin. *Carcinogenesis* 14(11):2353-2358.

27. Fujiwara K, Wie B, Elliott R, & Nagase H (2010) New outbred colony derived from Mus musculus castaneus to identify skin tumor susceptibility loci. *Mol Carcinog* 49(7):653-661.

28. Angel JM, Caballero M, & DiGiovanni J (2003) Identification of novel genetic loci contributing to 12-O-tetradecanoylphorbol-13-acetate skin tumor promotion susceptibility in DBA/2 and C57BL/6 mice. *Cancer Res* 63(11):2747-2751.

29. Gazin C, Wajapeyee N, Gobeil S, Virbasius CM, & Green MR (2007) An elaborate pathway required for Ras-mediated epigenetic silencing. *Nature* 449(7165):1073-1077.

30. Chida K, *et al*. (2003) Disruption of protein kinase Ceta results in impairment of wound healing and enhancement of tumor formation in mouse skin carcinogenesis. *Cancer Res* 63(10):2404-2408.

31. Wang X, *et al*. (2008) Screening of new tumor suppressor genes in sporadic colorectal cancer patients. *Hepatogastroenterology* 55(88):2039-2044.

Figure Legends

Figure 1. Generation of transgenic mice

A. Schematic diagram of PLCε showing domain organization. The underlined region at the N-terminus indicated by an asterisk represents a largely unstructured and evolutionary highly variable (in length and sequence) portion of PLCε that has not been removed using the strategy described in B (left).

B. Strategies for generation of *Plce1* null (left) and $Plce^{RAm/RAm}$ (right) alleles.

C. Number and percentage (%) of offsprings generated from $Plce^{+/-}$ (top) and $Plce^{+/RAm}$ (bottom) intercrosses, genotyped 3 weeks after birth.

D. Total RNA was extracted from $Plce^{+/+}$ and $Plce^{-/-}$ brain, heart, lung and skin and RT-PCR was performed using primers for exon 2-3 (left panel). Genomic DNA, extracted from brain, heart, lung and skin of $Plce^{+/+}$ and $Plce^{RAm/RAm}$ mice, was amplified (sequences flanking exons 29 and 30) by PCR and the product digested with HpaI or HaeIII (right panel).

Figure 2. Two-stage skin chemical carcinogenesis model applied to different *Plce* genotypes

A. Evaluation of PLCε expression in the skin of $Plce^{+/+}$, $Plce^{-/-}$, and $Plce^{RAm/RAm}$ mice. Quantitative RT-PCR (qRT-PCR) was performed using a probe made to hybridize with exon 2-3 of *Plce1*. Values were normalised to the expression level of the endogenous control, GAPDH. One-way ANOVA , * $P < 0.05$.

B. Cohorts of mice were treated with one application of DMBA and subsequent, twice a week applications of TPA for 18 weeks. Time course of the average number of tumours per mouse in FVB background (mean ± SEM) for $Plce^{+/+}$ (n= 33), $Plce^{-/-}$ (n=15) and $Plce^{RAm/Ram}$ (n=16) genotypes is shown per week after DMBA treatment. Two-way ANOVA, $P < 0.0001$.

C. Rate of tumour growth. The three greatest tumours of each animal were measured at 13 weeks after DMBA treatment and averaged per genotype; t-test, *P < 0.01.

D. Percentage of the survival rate per week after DMBA treatment for *Plce*$^{+/+}$, *Plce*$^{-/-}$, and *Plce*$^{RAm/RAm}$ mice.

E. Evaluation of epidermal hyperplasia in *Plce*$^{+/+}$, *Plce*$^{-/-}$, and *Plce*$^{RAm/RAm}$ mice. Dorsal skin of *Plce*$^{+/+}$ (n=7), *Plce*$^{-/-}$ (n=4), and *Plce*$^{RAm/Ram}$ (n=5) mice was treated with either acetone (Control, black) or TPA in acetone (TPA, grey); 48 hours after treatment the skin was excised, fixed and paraffin embedded. Proliferation was assessed by immunohistochemistry for Ki67, Ki67 positive cells were counted in 3 fields of view per skin sample. The data are shown as Mean ± SEM. Statistical analysis was performed using the student's t test: * P<0.05, ** P<0.01, ***P<0.0001.

Figure 3. Skin cancer model and PLCε downregulation

A. Evaluation of PLCε expression by qRT-PCR in normal skin (N) and tumour samples after 13 weeks of treatment (T) for indicated genotypes, normalised to expression of β-Actin (n=4 per genotype). Statistical analysis was by one-way ANOVA; ***P < 0.001 for *Plce*$^{+/+}$ and **P < 0.01 for *Plce*$^{RAm/RAm}$. Similar analysis did not reveal significant differences in expression levels of PLCδ1 (values within 100 ± 32) and PLCγ1 (values within 100 ± 26).

B. Evaluation of PLCε expression by qRT-PCR in *Plce*$^{+/+}$ and *Plce*$^{RAm/RAm}$ MEFs, normalised to the levels of expression of GAPDH. Primary MEFs were transfected with a retrovirus expressing the activated mutant HrasV12 (Hras) or a dominant negative form of the tumour suppressor protein p53 followed by a transfection with HrasV12 (p53DD+Hras), or the same backbone empty vector (empty vector). Results are representative for three different cell lines.

C. Evaluation of PLCε expression by qRT-PCR in non-transfected wild type, primary MEFs (primary) and these MEFs transfected with HrasV12 or p53DD+HrasV12, as described in B. In treated cells, the evaluation was performed three days after 15μM of DNA methylation inhibitor (AZA) treatment and 18hr after 400nM of histone deacetylase inhibitor (TSA) treatment. Results are representative for three different cell lines.

D. Evaluation of PLCε expression by qRT-PCR in untreated ventral skin (untreated skin), dorsal skin treated with DMBA-TPA for 13 weeks (treated skin) and two isolated tumours from the same mouse (tumour); analysis was performed on 3 mice (n=3). Statistical analysis was by one-way ANOVA, ***P < 0.001. As a further control, expression levels of PLCε were compared between untreated ventral (values 100 ±19) and untreated dorsal skin (values 115 ± 16), showing no difference.

Figure 4. NSCLC: LSL-*Kras*^{G12D} model and PLCε downregulation

A. Evaluation of PLCε expression by qRT-PCR in organs from wild-type mice (n=3) normalised to the levels of GAPDH; relative values compared to expression in the skin (skin=1).

B. *Plce*$^{+/+}$ (n=12), *Plce*$^{-/-}$ (n=12) and *Plce*$^{RAm/RAm}$ (n=11) mice carrying one LSL-KrasG12D allele were treated once with AdenoCre viruses by intranasal instillation. 23/24 weeks later, mice were sacrificed and the lungs processed for histological analysis. Quantification of the number of lesion per lungs is shown.

C. Quantification of the area of lesion per area of total lung in the indicated genotypes treated as described in B.

D. Quantification of the number of solid tumours of the mice of the indicated genotypes treated as described in B.

E. Assessment of the percentage of animals having solid tumours per indicated genotype treated as described in B.

F. Evaluation of PLCε expression by qRT-PCR in whole lungs from the wild type non-treated (control) and from treated animals after 26 weeks (treated); t-test, **P <0.001 (n=5).

G. Evaluation of PLCε expression by qRT-PCR in two independent populations of LSL-Kras^{G12D} MEFs infected with Adenovirus expressing either control GFP (AdGFP) or Cre-GFP (AdCreGFP) after 2, 4 and 6 days. Asterisks represent significant differences, t-test * P<0.05.

H. Cancer profiling array comparing lung samples isolated from normal and tumour tissues from the same patient (n=21). Hybridization with PLCε probe was normalised to hybridization to the ubiquitin probe.

J. Western blot showing the levels of PLCε expression in epithelial lung cancer cell lines A549, A427, H358, H460 and H727 (left panel). RT-PCR for expression of PLCε in H358 and H460 cells treated with 15μM AZA for three days and 400nM TSA for 18hr (right panel).

A

B

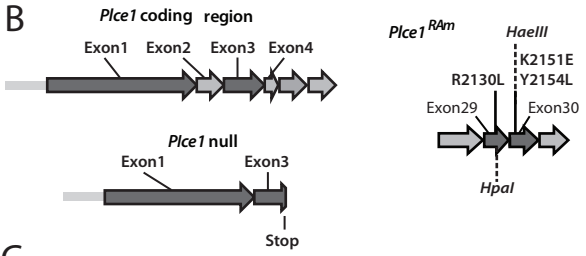

C

	Plce +/- x Plce +/-		
Plce	+/+	+/-	-/-
Mice	31 (25%)	66 (53%)	27 (22%)

	Plce +/RAm x Plce +/RAm		
Plce	+/+	+/RAm	RAm/RAm
Mice	18 (29%)	28 (46%)	15 (25%)

D

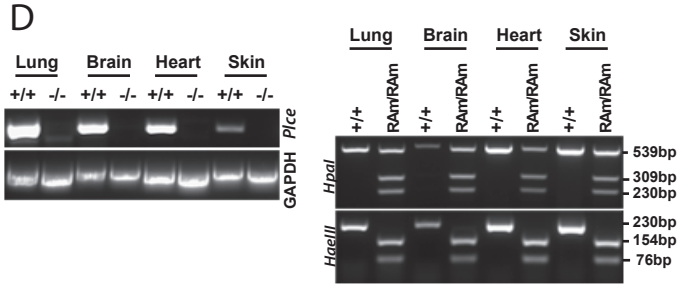

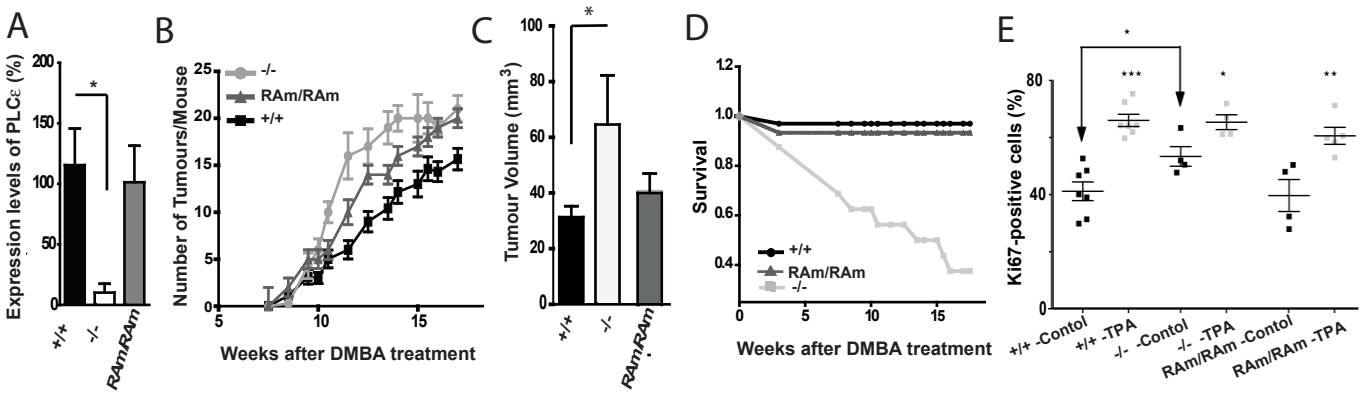
A
Expression levels of PLCε (%)
200
150
100
50
0
*
+/+
-/-
RAm/RAm
B
Number of Tumours/Mouse
25
20
15
10
5
0
-/-
RAm/RAm
+/+
5
10
15
Weeks after DMBA treatment
C
Tumour Volume (mm3)
100
80
60
40
20
0
*
+/+
-/-
RAm/RAm
D
Survival
1.2
1.0
0.8
0.6
0.4
+/+
RAm/RAm
-/-
0
5
10
15
Weeks after DMBA treatment
E
Ki67-positive cells (%)
80
40
0
*
***
*
**
+/+ -Contol
+/+ -TPA
-/- -Contol
-/- -TPA
RAm/RAm -Contol
RAm/RAm -TPA

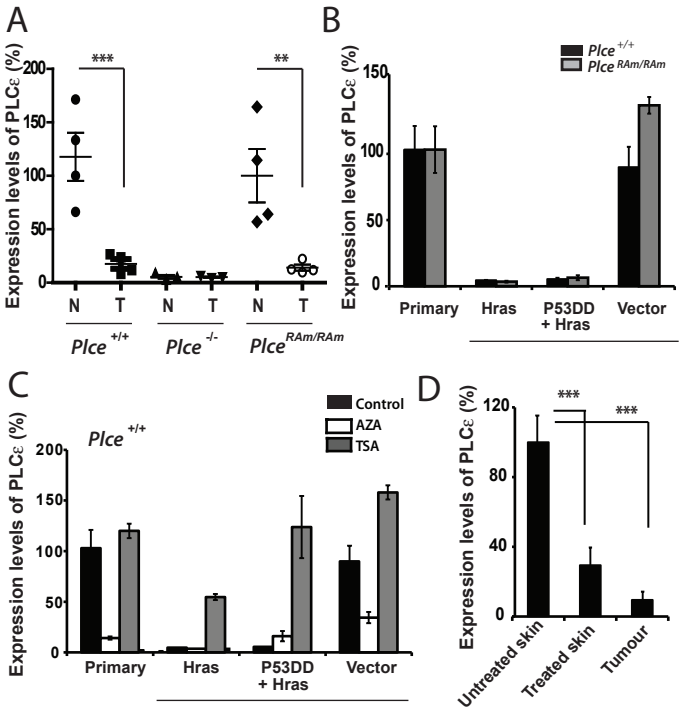
A
Expression levels of PLCε (%)
200
150
100
50
0
***
**
N
T
N
T
N
T
Plce +/+
Plce -/-
Plce RAm/RAm
B
Plce +/+
Plce RAm/RAm
Expression levels of PLCε (%)
150
100
50
0
Primary
Hras
P53DD + Hras
Vector
C
Control
AZA
TSA
Plce +/+
Expression levels of PLCε (%)
200
150
100
50
0
Primary
Hras
P53DD + Hras
Vector
D
Expression levels of PLCε (%)
120
80
40
0
***
***
Untreated skin
Treated skin
Tumour

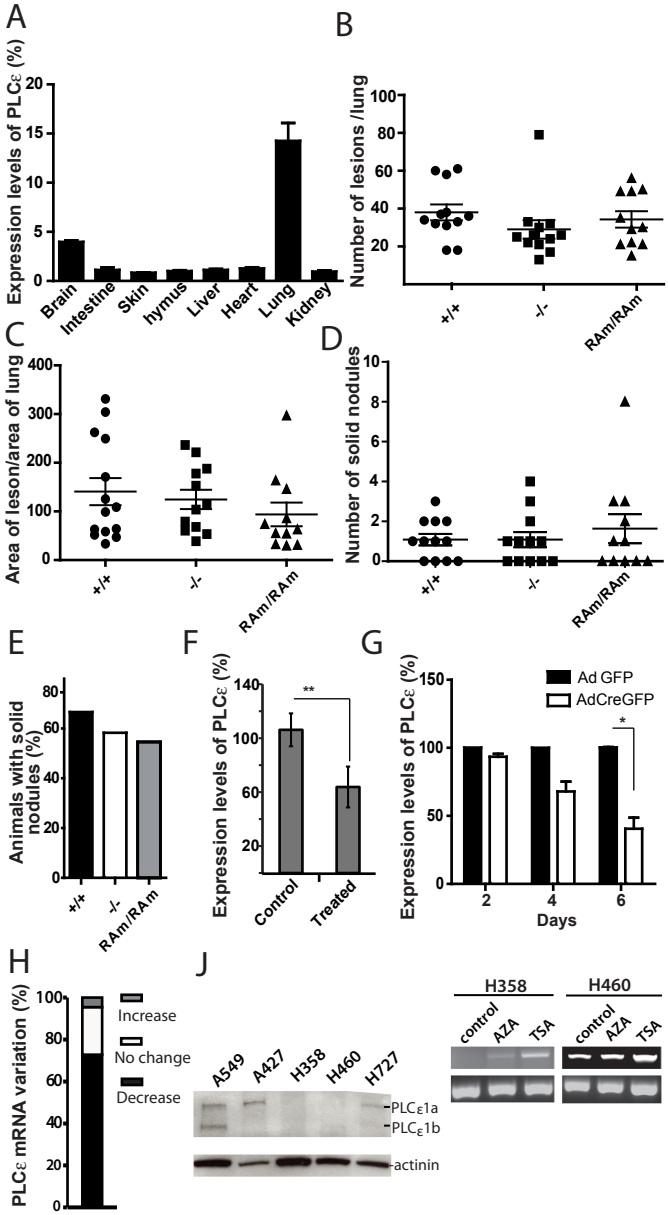
A
Expression levels of PLCε (%)
Brain
Intestine
Skin
hymus
Liver
Heart
Lung
Kidney
B
Number of lesions /lung
+/+
-/-
RAm/RAm
C
Area of leson/area of lung
D
Number of solid nodules
E
Animals with solid nodules (%)
F
Expression levels of PLCε (%)
Control
Treated
G
Expression levels of PLCε (%)
Ad GFP
AdCreGFP
Days
H
PLCε mRNA variation (%)
Increase
No change
Decrease
J
A549
A427
H358
H460
H727
PLCε1a
PLCε1b
actinin
H358
H460
control
AZA
TSA

SUPPLEMENTARY MATERIAL

Supplementary Materials and Methods

Viruses, plasmids and antibodies. Adenoviruses were obtained from the Gene Transfer Vector Core at the University of Iowa. Retroviruses of p53DD and HrasV12 as well as the pWZL-Neo retroviral vector used for exogenous expression of PLCε were from Addgene. Primary antibodies to PLCε, other PLC isoforms and Rap1 were as described in (1) and all antibodies to PKC enzymes and MARCKS proteins were from Cell Signalling except for generic anti-PKC antibody (Abcam, ab19031). Ki 67 antibody was from Abcam (ab16667).

Plce1 targeting constructs. *Plce1* is the only gene encoding PLCε enzyme and is denoted here as *Plce*. For the targeted deletion of *Plce*, DNA comprising exon2 of *Plce* was cloned into PGKNeo-F2L2DTA plasmid (Addgene plasmid 13445), upstream of the *PGK*-Neo selection cassette. The 5' short homology comprised of a 1.9kb fragment of DNA upstream of exon 2 and the 3' homology comprised of a 1.4 kb fragment downstream of exon 2. Diptheria toxin (DT) cassette was used as a negative selection marker; the construct was linearized using XhoI.

The knockin ($Plce^{RAm/RAm}$) targeting vector was generated by three point mutations (R2130L, K215E and Y2154L) in exon 29 and 30 of *Plce* shown to disrupt Ras binding (2). Exon 29 and 30 were then cloned into a modified version of *PGK*-Neo-F2L2DTA plasmid where one of the loxP sites was replaced by a polylinker and the other loxP site was mutated by deletion of three nucleotides. This construct was linearised with MluI.

Subsequently, 20μg of each construct was electroporated into Bruce 4 ES cells. The correctly targeted clones were identified by PCR. Southern blot analysis of the embryonic stem (ES) cells was used to confirm homologous recombination of the targeted allele and neomycin selection cassette was removed by crossing the $Plce^{-/-}$ and $Plce^{RAm/RAm}$ mice with transgenic mice carrying either a Cre- or Flp-recombinase under the *PGK* promoter, respectively. Clones were karyotyped by G banding of metaphase spreads and injected into albino C57BL/6J blastocysts.

All procedures involving animals were carried out under Home Office license authority and local Ethics Committee approval. Specific strains and number of crosses are indicated for each experimental procedure outlined below.

Skin Tumour Formation. C57BL/6J animals were backcrossed with FVB for 6 generations. A dorsal area of the skin of 8-week-old cohort mice was shaved and treated with a single application of 7.12-dimethylbenz(a)anthracene [DMBA (25ug in 100µl of acetone) Sigma] and subsequently treated with 12-O-tetradecanoyl-phorbor-13-acetate [TPA (0.2mmol/L in 100µl of acetone) Sigma] twice a week for 18weeks. Volume of the three largest tumours per animal was measured at week 13 after DMBA treatment.

The above procedure was also carried out using C57BL/6J wild-type animal crossed with DBA and three F1 C57BL/6J-DBA mice were treated as outlined. 13 weeks after DMBA treatment animals were sacrificed and treated (dorsal area), non-treated skin (ventral area) and two separate tumours were removed from each animal for analysis.

12-O-tetradecanoyl-phorbor-13-acetate induced skin hyperplasia. A dorsal area of the skin of F6 FVB 8-week-old mice was shaved and treated with either TPA (0.2mmol/L in 100µl of acetone) or vehicle (acetone); 48 hours after treatment TPA and vehicle treated areas of skin were excised, fixed in buffered formalin and embedded in paraffin. Overall morphology was assessed on hematoxylin and eosin (H&E) stained sections and proliferation was assessed by immunohistochemistry with Ki 67 antibody, counting three fields of view per animal.

Quantitative RT-PCR. RNA expression levels were determined by quantitative RT-PCR (qRT-PCR) using an ABI Prism 7700 Sequence Detection System (Applied Biosystems). Total RNA was extracted by RNeasy mini kit (Qiagen) following the manufacturer's protocol. Total RNA (1 μg) was reverse transcribed into cDNA using ImProm II Reverse Transcription System (Promega). Fluorogenic Taqman probes (catalog numbers Mm00457691_m1 for PLCε, 4352339E for GAPDH and 4352341E for β-Actin and TaqMan gene expression Master Mix (Applied Biosytems) were used for the qRT-PCR. The qRT-PCR product values obtained for PLCε were normalized

using those obtained for GAPDH in MEFs and mouse organs and β-Actin for tumour versus normal tissues.

Lung infection with adenovirus. The *LSL-Kras*^{G12D}mice were a generous gift of Dave Tuveson (3). The lung tumour experiments were performed on mice with a pure C57BL/6J genetic background. Briefly, the mice were anesthetized with ketamine and xylazine and treated once by intranasal instillation using $2x10^7$ pfu/mouse of AdCre viruses as described in (4). 23/24 weeks after AdCre infection (or as specifically indicated otherwise) animals were sacrificed, the lungs removed and the tumour burden and tissue analysed. Quantification of lesions was performed using Photoshop and ImageJ software of the scanned hematoxylin and eosin (H&E) stained lungs and areas were calculated in pixels.

Histopathology and immunohistochemistry. Skin was removed and fixed in 10% buffered formalin solution for 24hr. Lungs were perfused with PBS followed by fixation with 10% buffered formalin solution. Tissues were embedded in paraffin and gross morphology was assessed on H&E stained sections. Immunohistochemistry for Ki67 was performed using anti-Ki67 antibody (1:300). Apoptosis was measured on paraffin embedded tumour samples using an ApopTag Plus In Situ Apoptosis Detection Kit (Chemicon International, Temecula, CA).

In situ hybridization. *In situ* hybridization was carried out as previously described (5). To detect *Plce* transcripts two digoxigenin-labelled RNA probes were generated using in vitro RNA labelling Kit (Roche). Both probes, hybridizing respectively exon 1 to 3 and 6 to 8 of the wild-type PLCε RNA gave similar specificity.

Cell culture. MEFs were isolated from C57Bl/6J mouse embryos at 13.5 days of gestation as described in (1). Primary MEFs were immortalized by infection with retrovirus pBABE-Hygro p53DD (Addgene) and selected in Hygromycin B (Sigma) (200μg/ml) for over one week. Retrovirus infection of pBABE-Puro HrasV12 was performed on primary or immortalized p53DD MEFs and cells were selected at 2.5μg/ml of Puromycin (Sigma) for four days.

Primary LSL-Kras^{G12D} MEFs were transfected with AdCreGFP and AdGFP and total RNA was extracted 2, 4 and 6 days after adenovirus infection.

Culture of MEFs and NSLC cells lines A549 and A427 was performed in high glucose DMEM medium (Gibco) supplemented with 10% FBS and 2mM L-glutamine at 37ºC and 5% CO_2. NSLC cells lines H358, H460 and H727 were grown in RPMI medium (Gibco) supplemented with 10% FBS and 2mM L-glutamine at 37ºC and 5% CO_2.

Cancer profiling array. A commercial cancer profiling array I (Clontech BD Biosciences) was hybridized with radiolabeled DNA probes according to the manufacturer's instructions. Probes were generated as described in (6). RNA expression was quantified using a phosphorimager (Molecular Dynamics) and ImageQuant software; PLCε signal was normalized to ubiquitin signal.

Supplementary References

1. Martins M, *et al*. (2012) Activity of phospholipase C epsilon contributes to chemotaxis of fibroblasts towards platelet-derived growth factor. *J Cell Sci*.

2. Bunney TD, *et al*. (2006) Structural and mechanistic insights into ras association domains of phospholipase C epsilon. *Mol Cell* 21(4):495-507.

3. Tuveson DA, *et al*. (2004) Endogenous oncogenic K-ras(G12D) stimulates proliferation and widespread neoplastic and developmental defects. *Cancer Cell* 5(4):375-387.

4. DuPage M, Dooley AL, & Jacks T (2009) Conditional mouse lung cancer models using adenoviral or lentiviral delivery of Cre recombinase. *Nat Protoc* 4(7):1064-1072.

5. Rubin AN, *et al*. (2010) The germinal zones of the basal ganglia but not the septum generate GABAergic interneurons for the cortex. *J Neurosci* 30(36):12050-12062.

6. Sorli SC, Bunney TD, Sugden PH, Paterson HF, & Katan M (2005) Signaling properties and expression in normal and tumor tissues of two phospholipase C epsilon splice variants. *Oncogene* 24(1):90-100.

Supplementary Figures

Supplemental Figure S1. Verification of *Plce1* genotypes

A. Southern blotting of DNA fragments of a targeted ES cell line showing homologous recombination in the *Plce1* locus. After digestion of genomic DNA with SpeI, the generated probe hybridizes 11.2kb and 4.91Kb bands in the $Plce^{+/+}$ and $Plce^{-/-}$ targeted alleles, respectively. After DNA digestion with HpaI, the generated probe hybridizes 15.4kb and 6.73kb bands in the $Plce^{+/+}$ and $Plce^{RAm/RAm}$ targeted alleles, respectively.

B. Protein lysates from $Plce^{+/+}$ and $Plce^{-/-}$ MEFs were used to examine the level of expression of PLCε and other PLCs as indicated. 100μg of total protein lysate was used for Western blotting where α-actinin was used as loading control.

C. Evaluation of PLCε expression by qRT-PCR in the indicated organs from $Plce^{+/+}$, $Plce^{+/-}$ and $Plce^{-/-}$ mice (n=3 for each genotype); the data were normalised to the levels of GAPDH and the expression in $Plce^{+/+}$ genotype taken as a reference (100%). The evaluation was confirmed by Western blotting using anti-PLCε antibody (inset). Brain, heart, lung and intestine from $Plce^{+/+}$, $Plce^{+/-}$ and $Plce^{-/-}$ mice were isolated and 100μg of total protein lysates used for Western blotting. GAPDH was used as a loading control for all tissues.

Supplemental Figure S2. *In situ* hybridisation using PLCε probe in skin and lung sections.

In situ hybridization of wild type mice skin (**A**) and lung (**B**) is shown. Mice were anesthetized and transcardially perfused with 4% (w/v) paraformaldehyde (PFA) in PBS. Lung and skin were removed and immersed in 4% PFA overnight. Fixed

samples were cryoprotected and frozen on dry ice. Sections 20 μm in thickness were collected onto Superfrost Plus microscope slides. A DIG-labelled RNA probe hybridizing exon 6-8 was used to detect PLCe expression. Corresponding sense probe (right panels) was used as a control.

Supplemental Figure S3. PLCε in the skin and effects of its depletion in the two-stage chemical cancerogenesis model

A. Analysis of Hras mutations in skin tumours. Tumour DNA (T) was extracted and sequences flanking the 61st codon were amplified by nested PCR and analysed for a diagnostic fragment due to the sequence change; DNA from the tail was used as negative control (N); n=3 per indicated genotypes.

B. Dermis (D) and epidermis (E) from normal, non-treated (N) *Plce*$^{+/+}$mice were isolated and 200µg of total protein lysates used for Western blotting. Actin was used as a loading control (C).

C. Evaluation of apoptosis in skin tumours arising in *Plce*$^{+/+}$, *Plce*$^{-/-}$, and *Plce*$^{RAm/RAm}$ FVB mice after DMBA/TPA treatment. TUNEL-positive cells were measured in paraffin embedded tumour samples, using the ApopTag Plus In Situ Apoptosis Detection Kit. The total number of TUNEL-positive cells was quantified in six randomly selected microscopic fields of view at ×200 magnification. The data are presented as mean±SEM.

D. Time course of the average number of tumours per mouse (mean ± SEM), comparing *Plce*$^{+/+}$ and *Plce*$^{-/-}$ genotypes in a C57Bl/6J F1 mixed background (two-way ANOVA, P<0.0001).

E. Percentage of the survival rate per week after DMBA treatment of C57Bl/6J F1 mixed background mice, comparing *Plce*$^{+/+}$ and *Plce*$^{-/-}$ genotypes.

Supplemental Figure S4. TPA induced skin proliferation assessed using Ki67

For each condition, micrographs show overall morphology on H&E stained sections (left) and proliferation as assessed by Ki67 immunohistochemistry (right). Top,

vehicle and TPA treated skin of *Plce*$^{+/+}$; middle, vehicle and TPA treated skin of *Plce*$^{-/-}$; bottom, vehicle and TPA treated skin of *Plce*$^{RAm/Ram}$ mice. Scale bar represents 100μm.

Supplemental Figure S5. Expression levels of PLCε in cells undergoing different treatments

A. *Plce*$^{RAm/RAm}$ downregulation and re-expression after TSA treatment**.** Evaluation of PLCε expression by qRT-PCR in non-transfected (primary) *Plce*$^{RAm/RAm}$ MEFs and the *Plce*$^{RAm/RAm}$ MEFs transfected with HrasV12 and p53DD+HrasV12. Analysis of treated MEFs was performed three days after 15μM DNA methylation inhibitor (AZA) treatment and 18hr after 400nM histone deacetylase inhibitor (TSA) treatment. Results are representative for three different cell lines. Inset shows expression of Fas following AZA treatment.

B. *Plce*$^{+/+}$ MEFs were grown for 48 hrs (control, C) or made quiescent (Q) by growth to high cell density over 15 days with change of culture medium every 2 days (left). *Plce*$^{+/+}$ MEFs were grown under control conditions (C) or stimulated for 2 hrs with either 50 ng/ml PDGF-BB (T1) or 400 nM LPA (T2). Evaluation of PLCε expression by qRT-PCR was as in A.

C. Non transfected mouse epidermal keratinocyte cell line COCA (C, control) and COCA cells transfected with HrasV12 as described for MEFs (R) were evaluated for PLCε expression by qRT-PCR.

Supplemental Figure S6. Growth suppression by PLCε and downstream signaling

A. Effect of exogenous PLCε expression on growth of *Plce*$^{-/-}$ MEFs. *Plce*$^{-/-}$ transformed MEFs (p53DD+RasV12) were infected with retroviruses containing WZL-Neo vector (empty vector) or pWZL-Neo vector expressing wild-type PLCε (WT), lipase-inactive variant (Y1767A) and Ras-binding deficient variant (ΔRA2), as indicated in the top diagram. Following selection with G418 (600μg/ml) for two

weeks, the same number of cells was seeded and their growth evaluated after 3 days as shown in the bottom panel.

B. Effect of exogenous expression of PLCε on signaling in *Plce*$^{-/-}$ MEFs. *Plce*$^{-/-}$ transformed MEFs (p53DD+RasV12) infected with retroviruses containing WZL-Neo vector (vector) or with pWZL-Neo vector expressing wild-type PLCε (PLCε WT) were serum starved for 15 hrs and stimulated by 400 nM LPA (in a medium containing 5%FBS) for 2 minutes (left panels). Following this verification of reagents and methodology in a short stimulation, the control transformed MEFs (vector) and MEFs expressing PLCε (PLCε WT) were analysed when grown under conditions described in A, after 3 days of seeding (right panels).

Cell lysates (150 μg) were analysed by Western blotting using indicated antibodies with α-actinin as a loading control. For the analyses of GTP-bound state of Rap1, lysates were first incubated with GST-fusion RalGDS-RBD and the protein present in the "pull-down" subsequently analysed by Western blotting using antibodies to Rap1. The differences between the control MEFs (vector) and MEFs expressing PLCε (PLCε WT) in the levels of pPKC [using phospho-PKC (pan) antibodies] and the levels of pMARCKS were observed in three independent samples.

C. Control MEFs (vector) and MEFs expressing PLCε (PLCε WT) were analyzed as shown in B, right panels. Quantification of the bands corresponding to Rap1-GTP (top) and pPKC (bottom) was performed using ImageJ. The relative intensity in PLCε WT MEFs was set at 1 and used as a reference point. Asterisks represent significant differences, t-test ** $P<0.01$.

D. Evaluation of expression of PKC enzymes by qRT-PCR was performed in tumour samples generated by the two-stage chemical carcinogenesis protocol (after 13 weeks of treatment with DMBA) (T) and in corresponding samples from non-treated mice (N). Two genotypes were compared: *Plce*$^{+/+}$ (WT) and *Plce*$^{-/-}$ (KO), n=5 per genotype. Expression of PKCα, PKCη, PLCδ and PKCε was normalised to expression of β-actin and the values in the WT, non-treated samples (WT/N) for each isozyme used as a reference (100%) (top panel).

Western blotting was used to confirm protein expression using either a generic reagent cross-reacting with several PKC enzymes (PKC antibody) or the antibody to

PKCη, predominant in the normal skin (inset). The levels of pPKC were evaluated as described in C. Following quantification of the bands by ImageJ, the values were expressed as pPKC/actin ratio; for comparison of samples WT/N and KO/N, asterisk represent significant differences, t-test * $P<0.05$ (bottom panel).

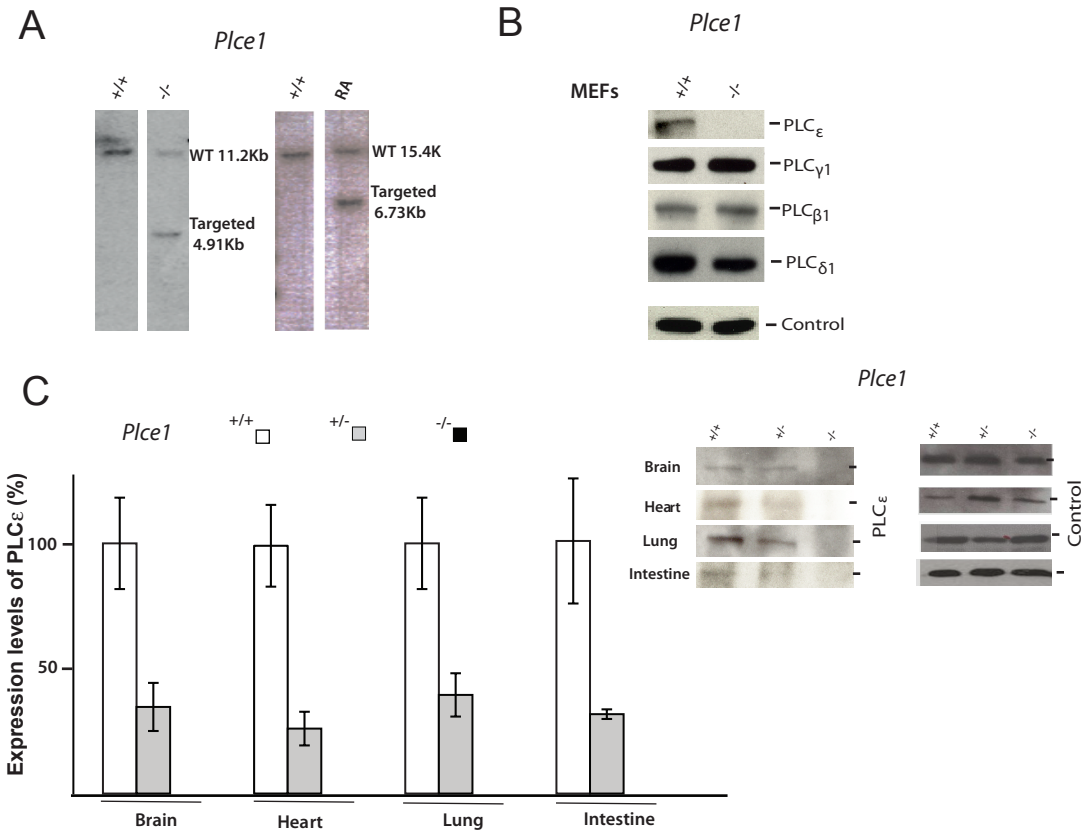
A
Plce1
+/+
-/-
WT 11.2Kb
Targeted
4.91Kb
+/+
RA
WT 15.4K
Targeted
6.73Kb
B
Plce1
MEFs
+/+
-/-
PLCε
PLCγ1
PLCβ1
PLCδ1
Control
C
Plce1
+/+
+/-
-/-
Expression levels of PLCε (%)
100
50
Brain
Heart
Lung
Intestine
Plce1
+/+
+/-
-/-
Brain
Heart
Lung
Intestine
PLCε
Control

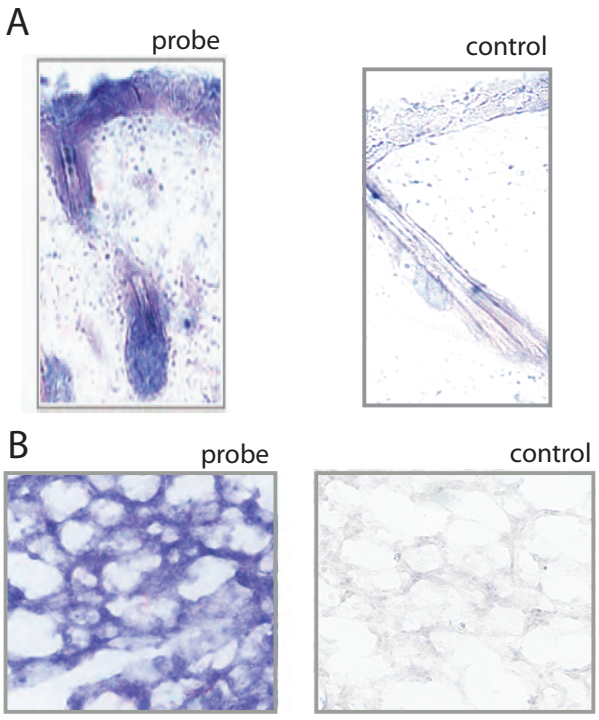
A
probe
control
B
probe
control

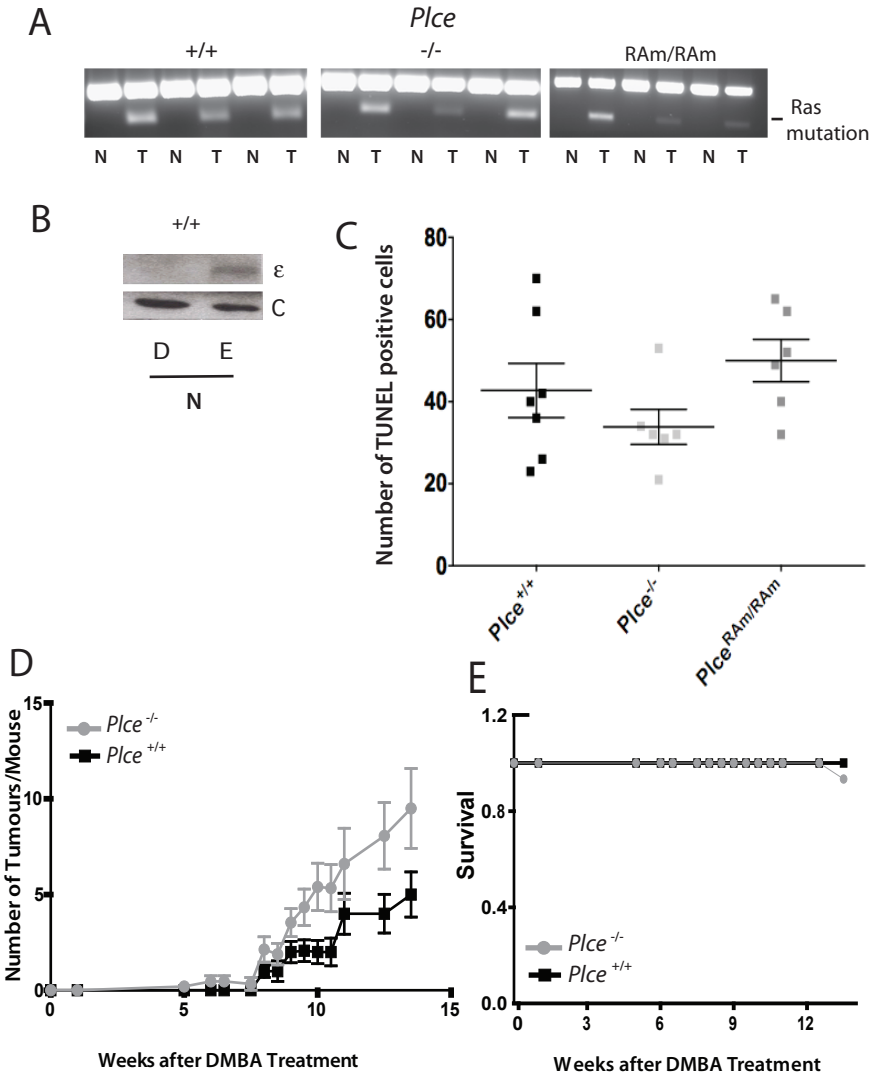
A
Plce
+/+
-/-
RAm/RAm
Ras mutation
N T N T N T N T N T N T N T N T N T
B
+/+
ε
C
D E
N
C
Number of TUNEL positive cells
80
60
40
20
0
Plce+/+
Plce-/-
PlceRAm/RAm
D
Number of Tumours/Mouse
15
10
5
0
Plce-/-
Plce+/+
0 5 10 15
Weeks after DMBA Treatment
E
Survival
1.2
0.8
0.4
0.0
Plce-/-
Plce+/+
0 3 6 9 12
Weeks after DMBA Treatment

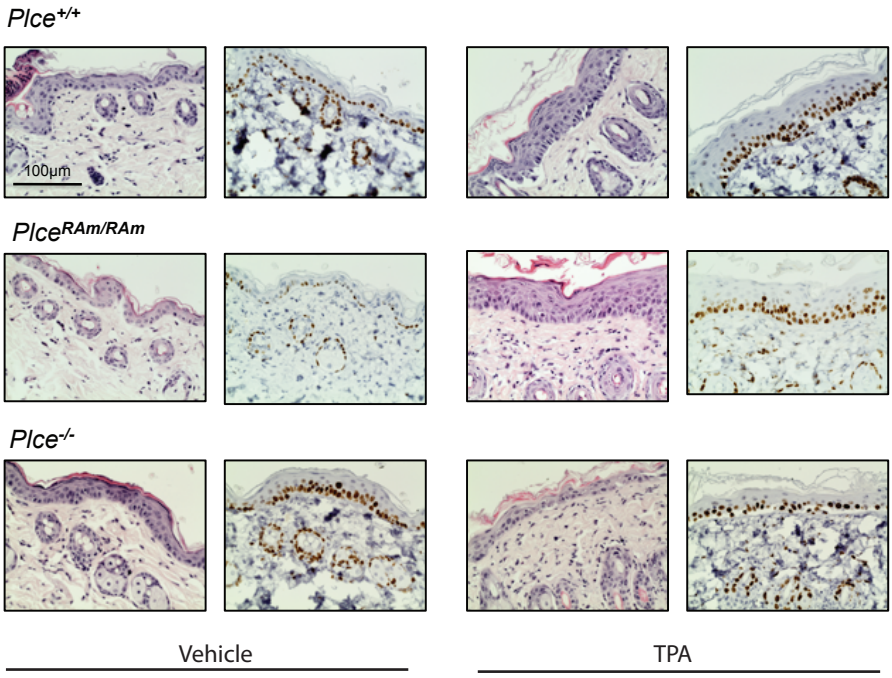
Plce+/+
100μm
PlceRAm/RAm
Plce-/-
Vehicle
TPA

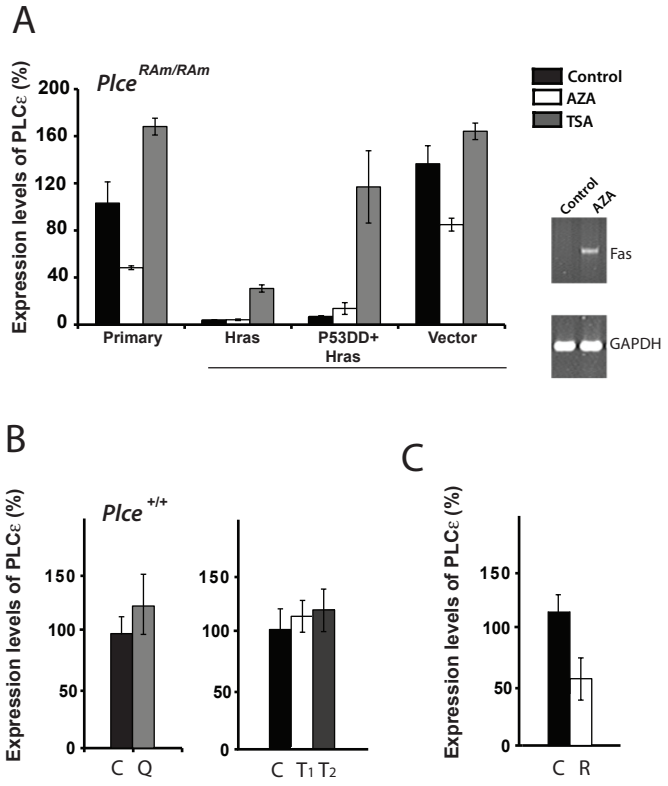
A
Plce RAm/RAm
Expression levels of PLCε (%)
200
160
120
80
40
0
Primary
Hras
P53DD+ Hras
Vector
Control
AZA
TSA
Control
AZA
Fas
GAPDH
B
Plce +/+
Expression levels of PLCε (%)
150
100
50
0
C Q
C T1 T2
C
Expression levels of PLCε (%)
150
100
50
0
C R

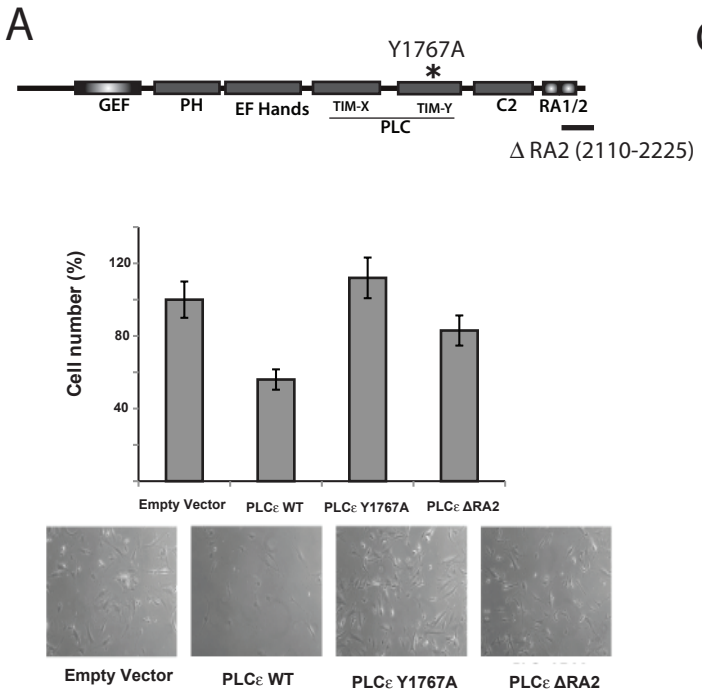
A
Y1767A
GEF
PH
EF Hands
TIM-X
TIM-Y
C2
RA1/2
PLC
Δ RA2 (2110-2225)
Cell number (%)
120
80
40
Empty Vector
PLCε WT
PLCε Y1767A
PLCε ΔRA2
Empty Vector
PLCε WT
PLCε Y1767A
PLCε ΔRA2

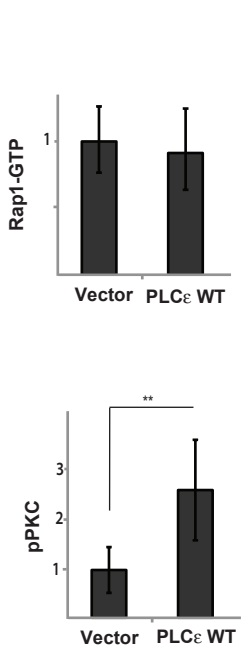
C
Rap1-GTP
1
Vector
PLCε WT
**
pPKC
3
2
1
Vector
PLCε WT

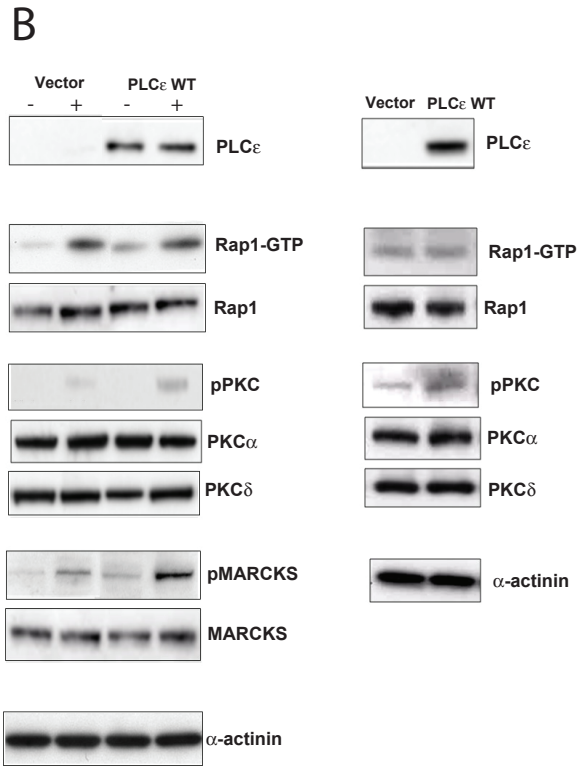
B
Vector
PLCε WT
- + - +
PLCε
Rap1-GTP
Rap1
pPKC
PKCα
PKCδ
pMARCKS
MARCKS
α-actinin
Vector PLCε WT
PLCε
Rap1-GTP
Rap1
pPKC
PKCα
PKCδ
α-actinin

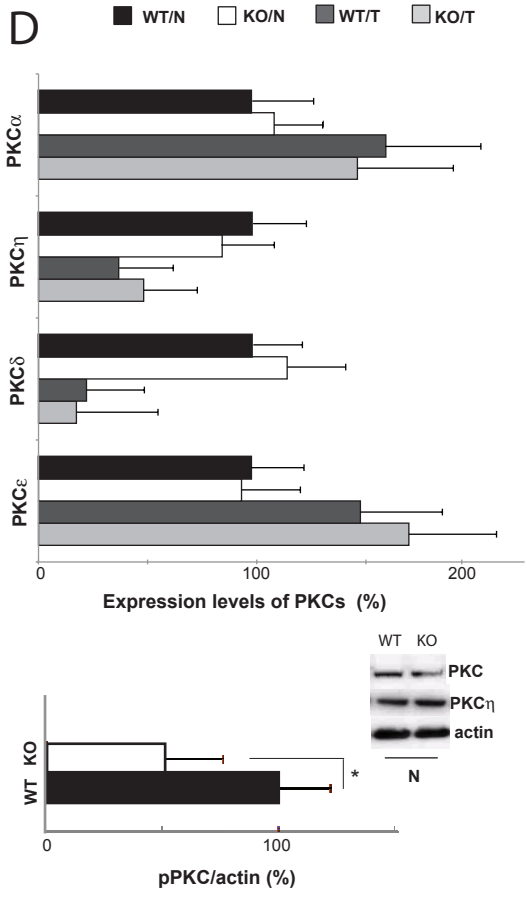
D
WT/N
KO/N
WT/T
KO/T
PKCα
PKCη
PKCδ
PKCε
0
100
200
Expression levels of PKCs (%)
WT KO
PKC
PKCη
actin
N
WT KO
*
0
100
pPKC/actin (%)